Hsp70 machinery vs protein aggregation

Serlidaki, Despina

DOI:
10.33612/diss.95000243

Chapter 3

Protein aggregation causes an aggregate-specific defect in cellular protein homeostasis

Despina Serlidaki, Margreet Koopman, Steven Bergink & Harm H. Kampinga

Department of Biomedical Sciences of Cells & Systems, University of Groningen,
University Medical Center Groningen,
Antonius Deusinglaan 1, 9713 AV, Groningen, The Netherlands.

Manuscript in preparation

Abstract

The protein quality control (PQC) network consists of a set of interconnected processes that ensure proper protein handling in order to maintain protein homeostasis in the cells. One of the purposes of a functional PQC network is the prevention of protein aggregation and its detrimental consequences, one of which is further protein homeostasis disruption. One of the possible hypotheses on how protein aggregation can impair protein homeostasis is the depletion or entrapment of crucial protein quality control components, like molecular chaperones. However, it is not clear in which way each aggregating protein affects protein homeostasis and if it influences the whole aggregation-prone proteome or only a subset of it. Therefore, we examined if different, non-interacting, disease-associated aggregating proteins, like polyglutamine proteins (polyQ) and mutant SOD1, can influence each other's aggregation. We show that polyQ aggregation enhanced mutant SOD1 aggregation but not vice versa, as polyQ aggregation remained unaltered despite the presence of mutant SOD1 aggregates. These data suggest that each aggregating protein generates a specific defect on protein homeostasis and not a generic system collapse.

Introduction

Protein homeostasis is portrayed as a balance between the efficiency of the protein quality control (PQC) components of a cell and the rate and quality of production, transport and remodelling of proteins (Balch et al., 2008). Proteotoxic stress conditions and/or genetic mutations increase metastable protein production thereby challenging protein homeostasis; if the PQC networks does not concomitantly adapt or if its total capacity declines, for example during aging, a collapse in protein homeostasis is imminent (Douglas and Dillin, 2010; Hipp et al., 2014; Kakkar et al., 2012; Kampinga and Bergink, 2016). Ineffective handling of metastable proteins typically leads to protein aggregation, a hallmark of many age-related neurodegenerative disorders including Alzheimer's, Parkinson's, amyotrophic lateral sclerosis (ALS) and polyglutamine (polyQ) diseases like Huntington's or spinocerebellar ataxias, with each disease involving different aggregation prone proteins (Ross and Poirier, 2004; Soto, 2003).

Aggregates can be toxic to the cells in many ways, likely depending on their structure and localization, for instance by interfering with the functions of essential cell components, like membranes (Lashuel and Lansbury, 2006; Bäuerlein et al., 2017), mitochondria (Lin and Beal, 2006; Hashimoto et al., 2003; Xie et al., 2010), nuclei (Woerner et al., 2016; Liu et al., 2015; Chou et al., 2018) or proteasomes (Bence et al., 2001; Bennett et al., 2005; Duennwald and Lindquist, 2008). In addition to that, sequestration of other metastable proteins within these aggregates can deprive the cell from proteins with essential functions (Olzscha et al., 2011). That is why cells have developed an elaborate PQC network of several systems to manage protein misfolding and prevent detrimental effects of protein aggregation (Chen et al., 2011; Tyedmers et al., 2010).

Molecular chaperones, and especially the HSP70 system, play a central role in all these different processes of the cellular PQC system (Bukau et al., 2006; Kim et al., 2013). With this in mind, it has been proposed that aggregates can trap and deactivate crucial PQC elements like chaperones, which are actually required to oppose such aggregate formation. This would initiate a progressive, self-perpetuating, decline in protein homeostasis, eventually even accelerating or inducing aggregation of aggregation prone proteins. The most compelling evidence for such a negative cascade was first provided by the lab of Morimoto, which showed that polyQ proteins in *C. elegans* disrupt protein folding and lead to aggregation of otherwise soluble structurally destabilized mutant proteins (Gidalevitz et al., 2006). Thereafter, more studies supported this using cellular models (Gupta et al., 2011) or different aggregation prone proteins like SOD1 (Gidalevitz et al., 2009).

Although components of the Hsp70 machinery, like HSP70s and HSP110s, have been found to be associated with aggregates of various proteins like mutant SOD1 (Wang et al., 2009), CFTR (Wigley et al., 1999), polyQ (Suhr et al., 2001; Kim et al., 2016; Wang et al., 2007) or artificial amyloid-like aggregates (Olzscha et al., 2011), there was no evidence in these studies that this chaperone recruitment by aggregates directly results in protein homeostasis defects. However, it has been shown that a-synuclein aggregates can interact with DNAJ co-chaperones and inhibit Hsp70 machinery function in vitro (Hinault et al., 2010). Moreover, by cellular experiments, it was demonstrated that polyQ protein aggregates can impede protein degradation by sequestering the HSP70 co-chaperone Sis1p/DNAJB1 (Park et al., 2013) and both polyQ and mutant SOD1 aggregates were found to inhibit HSP70-dependent clathrin-mediated endocytosis by recruiting and depleting HSPA8 (Yu et al., 2014).

However, are all types of aggregates equally disturbing in terms of their impact on PQC? And are all these aggregation-prone proteins equally potentiated by a depletion of PQC components caused by other aggregates? In fact, members of the Hsp70 system were found to be differently capable of processing various disease-associated aggregating proteins (Kakkar et al., 2014), suggesting a specificity in the chaperones needed for each aggregation-prone protein. We therefore hypothesized that entrapment and depletion of chaperones is a process that may differ per aggregating protein; thus, chaperone trapping by an aggregate may have a different impact on the aggregation propensity of other metastable proteins, depending on whether they are processed by the same chaperones or other PQC components or not. To test this hypothesis, we examined if independently aggregating proteins, like polyQ and ALS-causing mutant SOD1 (Matsumoto et al., 2006; Polling et al., 2014; Weisberg et al., 2012), that do not rely on the same set of chaperones for prevention of aggregation (Table S1), can influence each other's aggregation. Consistently with the proposed protein homeostasis models, we found that polyQ aggregation substantially enhanced mutant SOD1 aggregation but, on the contrary, aggregation of mutant SOD1 had no influence on the extent of polyQ aggregation.

Results

PolyQ and mutant SOD1 form different types of aggregates

In order to examine the impact of protein aggregation on cellular protein homeostasis, we aimed to test the effect of aggregation of one protein on the aggregation of a second protein and vice versa, with the prerequisite that these different aggregation prone proteins would not directly interact and co-aggregate with each other. Hereto we chose polyQ and

mutant SOD1 as our model proteins, since it has been shown that they form different types of aggregates with distinct molecular properties (Matsumoto et al., 2006) and at different positions in the same cell (Weisberg et al., 2012; Polling et al., 2014), suggesting they do not physically interact.

We used SOD1^{A4V}, a well-known mutant associated to familial ALS that causes aggregation of the protein (Prudencio et al., 2009; Ray et al., 2004; Chattopadhyay and Valentine, 2009),

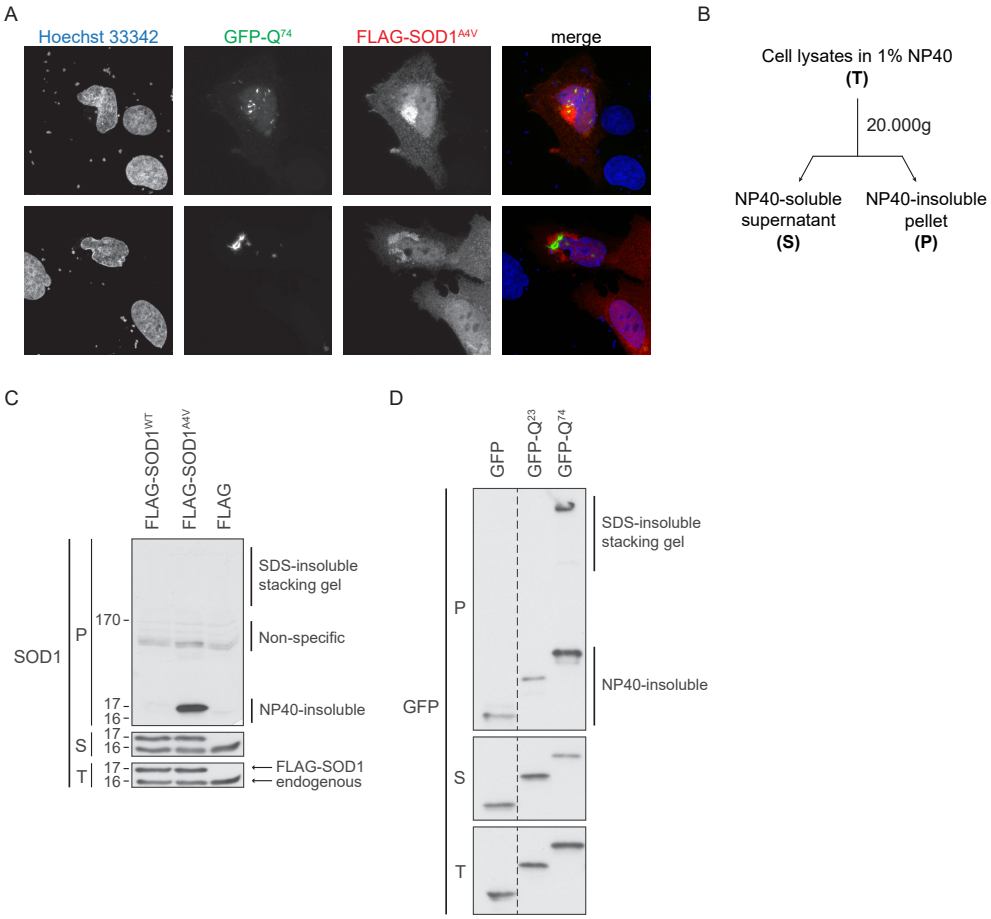

Figure 1. SOD1^{A4V} and polyQ form independent and biochemically different aggregates in the same cell. (A) U2OS cells co-expressing GFP-tagged Q74 (green) with FLAG-SOD1^{A4V} (red) for 48 hours detected by fluorescence confocal microscopy. FLAG-SOD1^{A4V} is stained anti-FLAG and Alexa 633 secondary antibody. Hoechst 33342 (blue) is used to stain nuclei. Maximum intensity projection of individual z-stacks is shown. **(B)** Scheme of NP40 fractionation protocol described in Materials and Methods. **(C-D)** NP40 fractionation of cells expressing **(C)** FLAG-tagged SOD1^{WT}, SOD1^{A4V} or empty FLAG vector or **(D)** GFP, GFP-Q^{23} or GFP-Q^{74}, both for 48 hours. Western blots with **(C)** SOD1 or **(D)** GFP antibodies of total cell lysates (T), NP40-soluble (S) or NP40-insoluble (P) fractions are shown. Stacking gel of (P) fraction is blotted for SDS-insoluble proteins.

and a Huntingtin exon 1 fragment with an expanded stretch of 74 glutamines (Q^{74}) that is known to form amyloid aggregates (Bates, 2003; Wyttenbach et al., 2000; Rujano et al., 2007; Michalik and Van Broeckhoven, 2003). Immunofluorescence experiments confirmed that GFP-tagged Q^{74} and FLAG-tagged $SOD1^{A4V}$ can aggregate independently at different positions within the same cell (Fig 1A). While GFP-Q^{74} usually formed one or more compact aggregates of high intensity, either nuclear or cytoplasmic or both, FLAG-$SOD1^{A4V}$ mostly formed one large diffuse aggregate next to the nuclear staining and there was little or no overlap between Q^{74} and $SOD1^{A4V}$ aggregates (Fig 1A), confirming previous studies (Matsumoto et al., 2006; Weisberg et al., 2012; Polling et al., 2014). Importantly, also the biochemical properties of Q^{74} aggregation were found to be distinct from that of $SOD1^{A4V}$; using the same NP40 detergent fractionation (Fig 1B) of cells expressing either of the two proteins for 48 hours, we noticed that Q^{74} formed 2% SDS-insoluble high molecular weight aggregates that were retained in the stacking gel during SDS-PAGE of the NP40-insoluble (P) fraction (Fig 1C) whilst $SOD1^{A4V}$ aggregates were SDS-soluble but could be detected as NP40-insoluble material (Fig 1D). At the same time, wild type SOD1 was only detected in the soluble (S) fraction (Fig 1C) together with the endogenous SOD1, confirming that the NP40-insoluble fraction represents aggregating mutant SOD1 species. Normal, non-aggregating polyQ with 23 glutamines (Q^{23}), like GFP control, did not form any SDS-insoluble aggregates and was mostly found in the NP40-soluble fraction but, possibly due to high expression levels, both Q^{23} and GFP were also sometimes detected in the NP40-insoluble fraction, although to a much lesser extend compared with Q^{74} (Fig 1D).

Q^{74} aggregation can enhance $SOD1^{A4V}$ aggregation but Q^{74} aggregation remains unaffected by $SOD1^{A4V}$

In order to analyse the effect of polyQ on mutant SOD1 aggregation, we co-expressed either GFP control, non-aggregating GFP-Q^{23} or aggregating GFP-Q^{74} together with either non-aggregating FLAG-$SOD1^{WT}$ or aggregating FLAG-$SOD1^{A4V}$. Whereas co-expression of Q^{23} with $SOD1^{A4V}$ had no significant effect on the extent of $SOD1^{A4V}$ aggregation, co-expression of Q^{74} significantly enhanced it (Fig 2A). Inversely, however, there was no effect of $SOD1^{A4V}$ on Q^{74} aggregation compared to $SOD1^{WT}$ as detected by the high molecular weight bands of GFP-Q^{74} (Fig 2A).

To confirm that the stacking gel retained material corresponded to SDS-insoluble aggregates, we used a filter trap assay to detect polyQ aggregates of GFP-Q^{23} or GFP-Q^{74} when co-expressed with either FLAG-tagged $SOD1^{WT}$ or $SOD1^{A4V}$. Similar to what we observed in the NP40 fractionation experiments (Fig 2A), there was no difference in Q^{74} aggregation detected by filter trap with either $SOD1^{WT}$ of $SOD1^{A4V}$ co-expression (Fig S1A). However, we did notice a small enhancement of Q^{74} aggregation when either $SOD1^{WT}$ or

SOD1^{A4V} were expressed compared to our control (Fig S1); since we used a FLAG-empty vector, which does not express any protein, as a control for the FLAG-tagged SOD1 proteins, this increase could correspond to the increased general protein levels compared to the control situation.

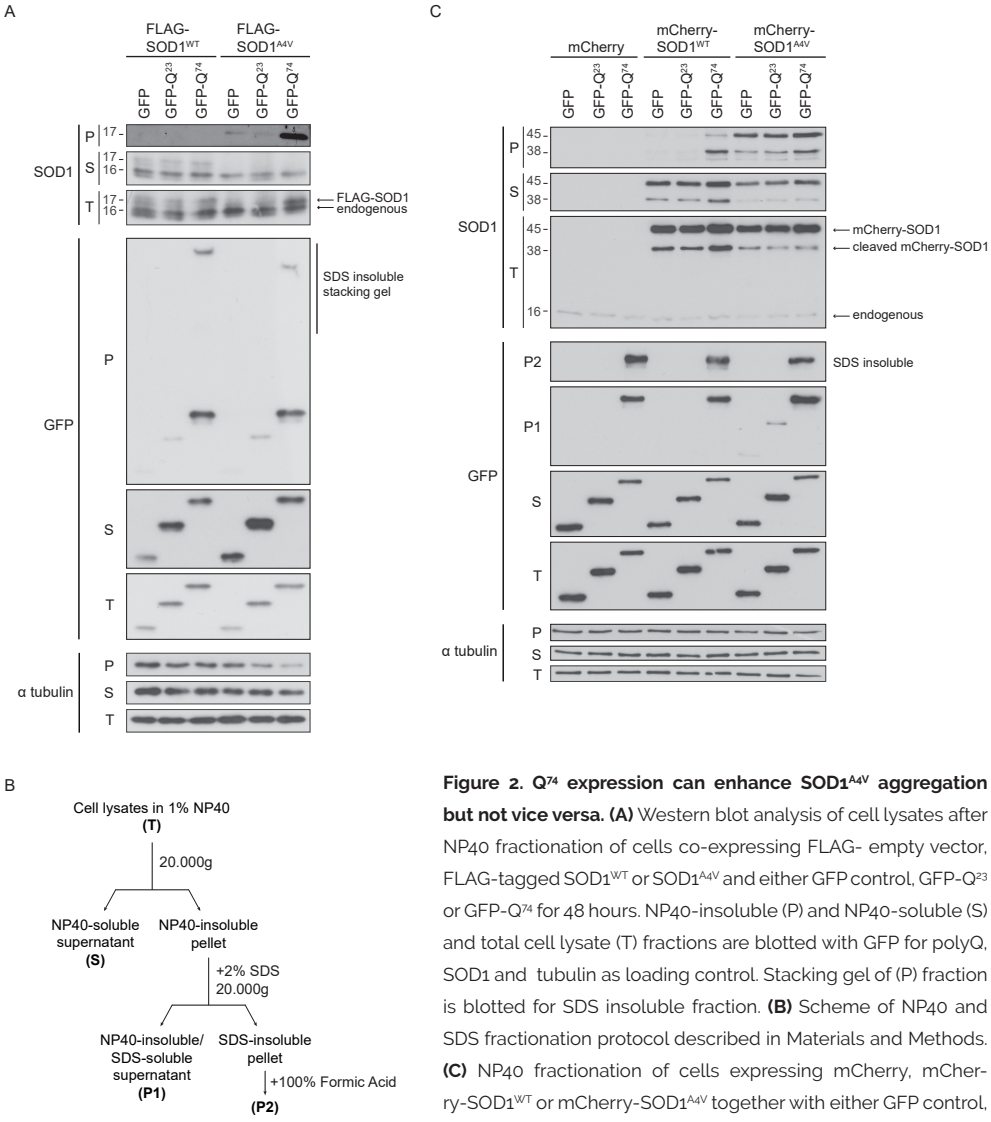

Figure 2. Q^{74} expression can enhance SOD1^{A4V} aggregation but not vice versa. (A) Western blot analysis of cell lysates after NP40 fractionation of cells co-expressing FLAG- empty vector, FLAG-tagged SOD1^{WT} or SOD1^{A4V} and either GFP control, GFP-Q^{23} or GFP-Q^{74} for 48 hours. NP40-insoluble (P) and NP40-soluble (S) and total cell lysate (T) fractions are blotted with GFP for polyQ, SOD1 and tubulin as loading control. Stacking gel of (P) fraction is blotted for SDS insoluble fraction. **(B)** Scheme of NP40 and SDS fractionation protocol described in Materials and Methods. **(C)** NP40 fractionation of cells expressing mCherry, mCherry-SOD1^{WT} or mCherry-SOD1^{A4V} together with either GFP control, GFP-Q^{23} or GFP-Q^{74} for 48 hours. GFP, SOD1 and tubulin –stained blots of total cell lysates (T), NP40-soluble (S), NP40-insoluble (P1) or SDS-insoluble (P2) fractions are presented.

To examine whether the lack of an effect of $SOD1^{A4V}$ on polyQ aggregation was due to relatively low expression levels of FLAG-SOD1, we used mCherry-tagged SOD1 constructs that can be expressed at higher levels than the FLAG-tagged constructs (compare Fig 2A & 2C: FLAG- and mCherry-tagged versions to endogenous SOD1 levels (16 kD band)). mCherry-SOD1 is detected as two bands on the western blot: a 45 kD band that corresponds to the full length fusion protein and a 38 kD band that correspond to a product of N-terminal cleavage of mCherry (Campbell et al., 2002; Gross et al., 2000) while still attached to SOD1 (Fig 2C). We then expressed mCherry control, mCherry-$SOD1^{WT}$ or mCherry$SOD1^{A4V}$ together with either GFP control, GFP-Q^{23} or GFP-Q^{74}. After 48 hours of expression, the cells were fractionated using the same NP40 fractionation as before; in addition, we included an extra 2%-SDS fractionation step after which, the pellet was solubilized with formic acid (Hazeki et al., 2000) yielding a separate SDS-insoluble fraction (P2) next to an NP40-insoluble, but SDS soluble, fraction (P1) from the supernatant (Fig 2B). We again observed no alteration in the Q^{74} SDS-insoluble (P2) fraction between co-expression with either mCherry-only, mCherry-$SOD1^{WT}$ or mCherry-$SOD1^{A4V}$ (Fig 2C). However, we did notice a minor increase in the NP40-insoluble (P1) fraction of GFP, Q^{23} and Q^{74} when co-expressed with $SOD1^{A4V}$ (Fig 2C), suggesting that $SOD1^{A4V}$ might induce some kind of oligomerization of these proteins without affecting the formation of SDS-insoluble aggregates. Overall, our data shown so far suggest that polyQ disturbs PQC components needed for $SOD1^{A4V}$ aggregation handling but not the other way around.

As seen before for FLAG-tagged $SOD1^{A4V}$, GFP-Q^{74} co-expression enhanced mCherry-$SOD1^{A4V}$ aggregation (Fig 1C); GFP-Q^{74} expression even shifted part of $SOD1^{WT}$ into the NP40-insoluble (P1) fraction (Fig 1C), which was previously undetected probably due to low expression of FLAG-$SOD1^{WT}$. This effect seemed to be Q length-dependent, as a longer polyQ of 119 glutamines (Q^{119}-YFP), with increased aggregation propensity (Rujano et al., 2007), induced a more prominent effect on $SOD1^{A4V}$ aggregation compared to Q^{74} (Fig S1B).

$SOD1^{A4V}$ expression does not even affect slowly aggregating Q^{43}

Since we observed no effect of $SOD1^{A4V}$ co-expression on polyQ^{74} aggregation, we hypothesized that the rate of Q^{74} aggregation might be faster than that of mutant SOD1, leaving no time for $SOD1^{A4V}$ to occupy or trap components important for polyQ aggregation. To test this hypothesis, we used a polyQ construct with 43 glutamines (Q^{43}) that aggregates slower than Q^{74} (Rujano et al., 2007). We co-expressed either GFP control, non-aggregating GFP-Q^{23} or slowly aggregating GFP-Q^{43} together with either non-aggregating mCherry-$SOD1^{WT}$ or aggregating mCherry-$SOD1^{A4V}$ for 48 hours. In such a scenario, Q^{43} did not enhance $SOD1^{A4V}$ aggregation levels (Fig 3), suggesting that polyQ aggregates only affect the rate of $SOD1^{A4V}$ aggregation if their formation preceded $SOD1^{A4V}$ aggregation, consistent

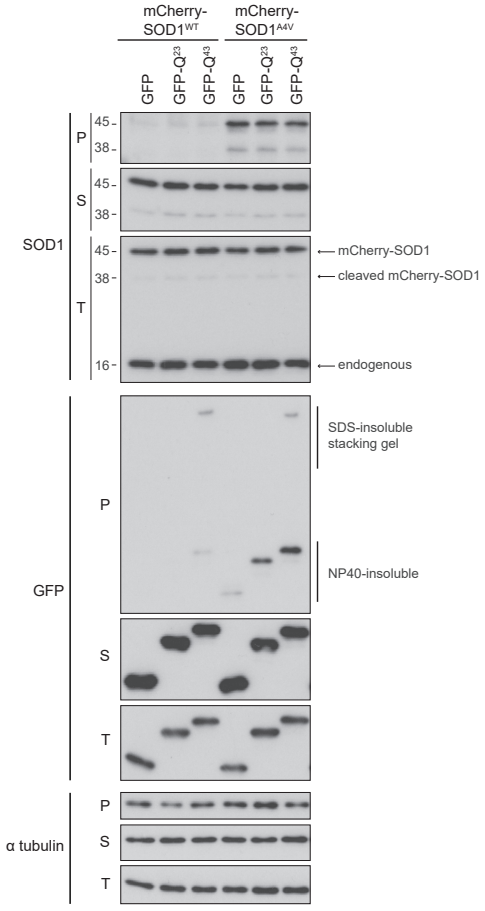

Figure 3. SOD1^{A4V} expression has no effect on slowly aggregating Q^{43} but increases SDS-soluble large oligomers. Western blots of NP40 fractionation of cell lysates collected 48 hours after transfection of cells with mCherry-SOD1^{WT} or mCherry-SOD1^{A4V} and either GFP, GFP-Q^{23} or GFP-Q^{43}. Total cell lysates (T), NP40-soluble (S) NP40-insoluble (P) were blotted with GFP, SOD1 or tubulin (loading control). Stacking gel of (P) fraction is blotted for SDS insoluble fraction.

with the idea that trapping is a late event during polyQ aggregate formation. That was confirmed by using an inducible HEK293 cell line, where we could co-transfect polyQ and SOD1 constructs and delay induction of SOD1 expression for 24 hours after transfection. In this way polyQ was expressed for 72 hours and SOD1 for 48 hours before NP40/SDS fractionation; in this case, we did observe an increase of SOD1^{A4V} aggregation when Q^{43} was co-expressed (Fig S2).

Similar to our observations for Q^{74}, however, Q^{43} SDS-insoluble aggregates were unaffected by SOD1^{A4V} expression (Fig 3), rejecting the hypothesis that the absence of an effect of SOD1^{A4V} on polyQ aggregation is caused by a slower speed of SOD1^{A4V} aggregation, but supporting the idea instead that SOD1^{A4V} does not trap PQC components crucial for dealing with polyQ aggregation. We again found an increase of the (P) fraction of all GFP constructs for not only Q^{43} and Q^{23} but also free GFP, when co-expressed with SOD1^{A4V} (Fig 3), suggesting that SOD1^{A4V} might occupy some PQC elements important for dissociation of larger, non-aggregating, oligomeric protein species that do not seem to be related to aggregate formation.

Discussion

Our data demonstrate that different aggregates do not have the same impact on protein homeostasis and sometimes but not always alter the subsequent aggregation propensity of other aggregation-prone proteins. PolyQ and mutant SOD1 have been manifested

to form structurally different types of aggregates. PolyQ proteins form dense amyloid aggregates, and other proteins and chaperones are mostly recruited around them (Kim et al., 2016; Matsumoto et al., 2006; Gillis et al., 2013). On the other hand, mutant SOD1 forms diffuse porous aggregates where other proteins and chaperones can move through and may not be irreversibly trapped (Matsumoto et al., 2006, 2005). The differences in aggregate structure are reflected as a different sensitivity to biochemical solubilization: polyQ fibrillar aggregates are resistant to strong ionic detergents like SDS (Fig 1D & (Hazeki et al., 2000)) whereas $SOD1^{A4V}$ are SDS-soluble and only resistant to mild, non-ionic, detergents like NP40 (Fig 1C & (Prudencio et al., 2009; Qualls et al., 2013)). Moreover, mutant SOD1 and polyQ mostly form aggregates at distinct positions in the cell; while polyQ forms either cytoplasmic aggregates of IPOD-like structures away from the nucleus or intranuclear aggregates, mutant SOD1 forms JUNQ/INQ/aggresome-like structures in the vicinity of the nucleus and the microtubule organizing center (Fig 1A) (Weisberg et al., 2012; Tyedmers et al., 2010; Bagola and Sommer, 2008; Miller et al., 2015a). All these converge to the conclusion that polyQ and mutant SOD1 aggregate independently in the cell and there is no direct interaction between these proteins. Therefore, these two proteins are most likely not "seeding" each other's aggregation directly. This is also supported by the fact that we only observe a one-sided effect - polyQ influencing mutant SOD1 aggregation - but not the other way around; on the contrary, in a cross-seeding situation, aggregation of both proteins should have increased.

Although $SOD1^{A4V}$ and polyQ aggregates are mostly aggregating independently, we observed that at very late stages of polyQ (Q^{74}) aggregation, when big aggregates with high intensity are formed, $SOD1^{A4V}$ is sometimes recruited around them forming a ring-like structure (Fig S3), like previously observed for chaperones and other proteins (Kim et al., 2016; Matsumoto et al., 2006; Gillis et al., 2013). Although we cannot rule out that $SOD1^{A4V}$ is actually co-aggregating at the surface of polyQ inclusions, hereby leading to the increase in $SOD1^{A4V}$ aggregation by the polyQ co-expression (Fig 2, S1), we rather interpret these (rare) features as a co-migration of (independently formed) polyQ aggregates at IPOD-like structures and $SOD1^{A4V}$ aggregates at the aggresome/JUNQ/INQ structures (Weisberg et al., 2012; Polling et al., 2014). Alternatively, the merging of these two different aggregates may have been mediated via interaction with other proteins or PQC components, for example chaperones or proteasomal degradation components which are known to be attracted by polyQ aggregates (Kim et al., 2016; Gillis et al., 2013), and $SOD1^{A4V}$ may be co-recruited there while still in interaction with these components. However, further investigation is needed in order to confirm that this ring-like structure around polyQ aggregates is indeed formed by aggregating species of $SOD1^{A4V}$.

So, why do polyQ aggregates enhance aggregation of $SOD1^{A4V}$ and why is the reverse effect not observed (Fig 2, 3 & S1)? We would like to speculate that polyQ aggregates are depleting some PQC components that are needed for handling mutant SOD1. Interestingly, co-expression of Q^{74} or Q^{119} not only increase aggregation but also expression levels of $SOD1^{A4V}$ and sometimes $SOD1^{WT}$ (Fig 2, S1, S2) and, at high $SOD1^{WT}$ expression levels, even shifted part of $SOD1^{WT}$ into the NP40-insoluble fraction (Fig 2B). This suggests that polyQ aggregates may impair PQC components that can normally assist in SOD1 proteasomal degradation; indeed, e.g. HSP70 (HSPA1A) or DNAJB1 are often found trapped in polyQ aggregates (Kim et al., 2016; Park et al., 2013) and they have been found to prevent aggregation of mutant SOD1 in a manner that is associated with reduced SOD1 expression levels (**Chapter 2** & (Koyama et al., 2006; Takeuchi et al., 2002)). Interestingly, a recent study showed that misfolded SOD1A4V is recruited and aggregates into compartments like stress granules, which contain many RNA-binding, aggregation-prone, proteins, and without direct interaction alters their dynamics (Mateju et al., 2017). This process seemed to be related to Hsp70 availability, which was also recruited there, suggesting that the stress granule formation, that require Hsp70 for their disassembly, may generate an Hsp70 shortage that increases SOD1 aggregation.

PolyQ aggregation, on the other hand, seemed to be largely unaffected by the presence of $SOD1^{A4V}$ aggregates (Fig 2 & 3), implying that mutant SOD1 aggregates either trap PQC components that are not in limited quantities in the cell or that they do not trap PQC components that are crucial for cellular handling of polyQ proteins, e.g. DNAJB6 (Hageman et al., 2010; Kakkar et al., 2016b), or do not trap chaperones/PQC components at all. The latter would be supported by the fact that SOD1 aggregates have a porous structure that is permissive for dynamic exchange of proteins within these aggregates (Matsumoto et al., 2006, 2005).

To conclude, aggregation of a protein not only influences the protein itself but can indirectly increase the possibility of aggregation of other aggregation-prone proteins that depend on the same PQC components. However, our data support the notion that protein aggregation does not cause a generic collapse in the protein homeostasis network of the cell but rather a specific breakdown that could potentially be restored if the PQC components involved would be replenished.

Materials and Methods

Cell culture, transfection and plasmids

Human osteosarcoma (U2OS) and human embryonic kidney (HEK293) stably expressing the tetracycline repressor (Flp-In-T-Rex HEK293, Invitrogen) cells were cultured using standard protocols in DMEM (Gibco) supplemented with 10% fetal bovine serum (Greiner Bio-One) and penicillin/streptomycin (Gibco). Cells were transiently transfected with Lipofectamine 2000 (Invitrogen) according to manufacturer's instructions. Expression in HEK293 cells was induced by 1ug/ml tetracycline. pEBB-FLAG-SOD1^{WT} and SOD1^{A4V} plasmids were a kind gift from Dr. B. van der Sluis (University Medical Center Groningen, NL) and described previously (Vonk et al., 2014). removing GFP from pcDNA5- FRT/TO-GFP-SOD1WT (described below) with HindIII/EcoRV digestion and substituting it with mCherry that was amplified from pcDNA3.1(+)-mCherry-alpha-tubulin (kind gift from Dr. B. Giepmans, University Medical Center Groningen, NL), using the primers described in Table S2, creating HindIII-mCherry-EcoRV and digested with HindIII/EcoRV as well. pcDNA5-FRT/TO- GFP-SOD1WT was generated by amplifying SOD1WT from the pEBB-FLAG-SOD1WT plasmid by using the primers described in Table S2 to generate EcoRV-XhoI-SOD1-BamHI-NotI and insert it after digestion with EcoRV/NotI into a pcDNA5-FRT/TO-GFP-no-stop plasmid (Hageman et al., 2010). pcDNA5-FRT/TO-mCherry-SOD1^{A4V} construct was generated by QuikChange XL Site-Directed Mutagenesis Kit (Agilent) from pcDNA5-FRT/TO-mCherry-SOD1^{WT} using the primers described in Table S2. pcDNA5-FRT/TO-GFP-stop, pEGFP-Q^{23} and -Q^{74}, p-Q^{119}-EYFP were described previously (Hageman et al., 2010). pcDNA3-FLAG-C1 (Addgene) was used as control.

NP40 and SDS fractionation

48 hours (or 72 hours when mentioned for Q^{43} experiments) after transfection, cells were washed with PBS and harvested in NP40 lysis buffer containing 50 mM Tris-HCl pH 8, 150 mM NaCl, 1 mM EDTA, 1% NP40 (Igepal-CA 630, Sigma) and complete protease inhibitor cocktail (Roche). Cell lysates were sonicated (50% input for 5 seconds), protein concentrations were measured with DC protein assay (Bio-Rad), equalized and a part was kept as the total (T) fraction representation. The remaining samples were centrifuged at 20000 g for 30 minutes at 4°C and NP40-soluble supernatant was kept separately as the (S) fraction. The pellet was washed once with lysis buffer and after another centrifugation at 20000 g for 30 minutes, supernatant was discarded and the pellet was resuspended in 1/3 of initial volume lysis buffer with sonication (50% input for 5 seconds), representing the NP40-insoluble (P) fraction. In all three fractions (T, S, P), 4x Laemmli buffer (8% SDS, 40% glycerol, 20% 2-mercaptoethanol, 0.001% bromophenol blue) was added and samples were

boiled for 5 minutes and kept at -20°C until use. When SDS fractionation was subsequently performed after NP40 fractionation, the (P) fraction was instead resuspended in 60 ul SDS buffer containing 50 mM Tris-HCl pH 8, 150 mM NaCl, 1 mM EDTA, 1% NP40 (Igepal-CA 630, Sigma), 2% SDS and 5% 2-mercaptoethanol. Samples were boiled for 10 mins, then centrifuged at 20000 g for 30 minutes at room temperature and supernatant was transferred in a new tube representing the NP40-insoluble fraction (P1). Pellet was washed once with SDS buffer and centrifuged again at 20000 for 30 minutes. The second pellet was resuspended in 20ul formic acid and, after a 30-minute incubation at 37°C, formic acid was removed by using vacuum concentrator at room temperature overnight. Dry pellet was resuspended in 1x Laemmli buffer, representing SDS-insoluble fraction (P2). In both P1 and P2 fractions, 0.001% bromophenol blue was added and samples were kept at -20°C until use.

Filter trap assay (FTA)

48 hours after transfection, cells were recovered by washed and recovered by either trypsinization or scraping in cold PBS, centrifuged at 3800 g for 3 minutes. Cell pellets were lysed in RIPA buffer [25 mM Tris-HCl pH 7.6, 150 mM NaCl, 1% NP40 (Igepal CA-630, Sigma), 1% sodium deoxycholate, 2% SDS, complete protease inhibitors cocktail (Roche)] and sonicated (50% input for 5 seconds). Protein concentrations were determined using DC protein assay (Bio-Rad). Concentrations were equalized and a part of each sample was kept separately, diluted 1:1 with 2x Laemmli buffer (125mM Tris-HCl pH 6.8, 4% SDS, 20% glycerol, 20% 2-mercaptoethanol, 0.001% bromophenol blue) and boiled for 5 minutes for western blot. The remaining part was diluted in FTA buffer (10 mM Tris-HCl pH 8.0, 150 mM NaCl and 50 mM dithiothreitol, 2% SDS), boiled for 5 minutes and prepared in three 5-fold serial dilutions into a final of 1x, 5x and 25x diluted samples for filter trap assay (FTA). FTA samples were loaded onto a 0.2 µm pore size cellulose acetate membrane prewashed with 0.1% SDS-containing FTA buffer. Membranes were washed three times with 0.1% SDS-containing FTA buffer, blocked with 10% non-fat milk and blotted with anti-GFP/YFP (JL-8, Clontech). After HRP-conjugated secondary antibody (Amersham) incubation, visualization was performed using enhanced chemiluminescence and Hyperfilm (ECL, Amersham).

Western blot and antibodies

Equal amounts of proteins were loaded into 12% SDS-PAGE gels. Proteins were transferred onto nitrocellulose membranes and blotted with the primary antibodies: GFP/YFP (JL-8, Clontech); FLAG (M2, Sigma); GAPDH (10R-G109A, Fitzgerald); SOD1 (FL-154, Santa Cruz); alpha-tubulin (T5168, Sigma); beta-actin (8H10D10, Cell Signaling). After incubation with the appropriate HRP-conjugated secondary antibody (Amersham), visualization was performed with enhanced chemiluminescence and Hyperfilm (ECL, Amersham).

Immunofluorescence and microscopy

48 hours after transfection, cells grown on coverslips were fixed using 3.7% formaldehyde in PBS for 15 minutes, washed three times with PBS, permeabilized with 0.2% Triton X-100 in PBS, incubated with 10mM glycine in PBS for 10 minutes and blocked with 3% BSA in PBS for 30 minutes. Coverslips were incubated with anti-FLAG (Sigma) primary antibody at 4°C overnight, washed again three times with PBS and incubated with Alexa Fluor 633 (Invitrogen) secondary antibody for 1-2 hours. Nuclei were stained with 0.2 µg/ml DAPI in PBS for 10 minutes. Microscopy was performed with a Leica TCS SP2 confocal microscope and image processing was done with ImageJ (NIH, https://imagej.nih.gov/ij/).

Acknowledgements

We would like to thank Dr. Bart van der Sluis (University Medical Center Groningen, NL) for the FLAG-SOD1 (WT and A4V mutant) constructs, Dr. Ben Giepmans (University Medical Center Groningen, NL) for the mCherry-containing plasmid and Jeanette Brunsting for her help with sub-cloning SOD1 constructs. Microscopy was performed at the UMCG Imaging and Microscopy Center (UMIC). This work was supported by the Research School of Behavioural and Cognitive Neurosciences (BCN) of the University of Groningen.

Author contributions

DS & MK performed the experiments. DS & HHK designed the experiments. SB and HHK supervised the experiments. DS & HHK analyzed the data and wrote the manuscript.

References

Bagola, K., and T. Sommer. 2008. Protein Quality Control: On IPODs and Other JUNQ. Curr. Biol. 18:1019–1021. doi:10.1016/j.cub.2008.09.036.

Balch, W.E., R.I. Morimoto, A. Dillin, and J.W. Kelly. 2008. Adapting Proteostasis for Disease Intervention. Science. 319:916–919. doi:10.1126/science.1141448.

Bates, G. 2003. Huntingtin aggregation and toxicity in Huntington ' s disease. Lancet. 361:1642–1644. doi:10.1016/S0140-6736(03)13304-1.

Bäuerlein, F.J.B., I. Saha, A. Mishra, M. Kalemanov, A. Martínez-Sánchez, R. Klein, I. Dudanova, M.S. Hipp, F.U. Hartl, W. Baumeister, and R. Fernández-Busnadiego. 2017. In Situ Architecture and Cellular Interactions of PolyQ Inclusions. Cell. 171:179–187. e10. doi:10.1016/j.cell.2017.08.009.

Bence, N.F., R.M. Sampat, and R.R. Kopito. 2001. Impairment of the Ubiquitin-Proteasome System by Protein Aggregation. Science. 292:1552–1555. doi:10.1126/science.292.5521.1552.

Bennett, E.J., N.F. Bence, R. Jayakumar, and R.R. Kopito. 2005. Global Impairment of the Ubiquitin-Proteasome System by Nuclear or Cytoplasmic Protein Aggregates Precedes Inclusion Body Formation. Mol. Cell. 17:351–365. doi:10.1016/j.molcel.2004.12.021.

Bukau, B., J. Weissman, and A. Horwich. 2006. Molecular Chaperones and Protein Quality Control. Cell. 125:443–451. doi:10.1016/j.cell.2006.04.014.

Campbell, R.E., O. Tour, A.E. Palmer, P.A. Steinbach, G.S. Baird, D.A. Zacharias, and R.Y. Tsien. 2002. A monomeric red fluorescent protein. Proc. Natl. Acad. Sci. U. S. A. 99:7877–82. doi:10.1073/pnas.082243699.

Chattopadhyay, M., and J.S. Valentine. 2009. Aggregation of Copper–Zinc Superoxide Dismutase in Familial and Sporadic ALS. Antioxid. Redox Signal. 11:1603–1614. doi:10.1089/ars.2009.2536.

Chen, B., M. Retzlaff, T. Roos, and J. Frydman. 2011. Cellular strategies of protein quality control. Cold Spring Harb. Perspect. Biol. 3:1–14. doi:10.1101/cshperspect.a004374.

Chou, C.-C., Y. Zhang, M.E. Umoh, S.W. Vaughan, I. Lorenzini, F. Liu, M. Sayegh, P.G. Donlin-Asp, Y.H. Chen, D.M. Duong, N.T. Seyfried, M.A. Powers, T. Kukar, C.M. Hales, M. Gearing, N.J. Cairns, K.B. Boylan, D.W. Dickson, R. Rademakers, Y.-J. Zhang, L. Petrucelli, R. Sattler, D.C. Zarnescu, J.D. Glass, and W. Rossoll. 2018. TDP-43 pathology disrupts nuclear pore complexes and nucleocytoplasmic transport in ALS/FTD. Nat. Neurosci. 21:228–239. doi:10.1038/s41593-017-0047-3.

Douglas, P.M., and A. Dillin. 2010. Protein homeostasis and aging in neurodegeneration. J. Cell Biol. 190:719–729. doi:10.1083/jcb.201005144.

Duennwald, M.L., and S. Lindquist. 2008. Impaired ERAD and ER stress are early and specific events in polyglutamine toxicity. Genes Dev. 22:3308–3319. doi:10.1101/gad.1673408.

Gidalevitz, T., A. Ben-Zvi, K.H. Ho, H.R. Brignull, and R.I. Morimoto. 2006. Progressive disruption of cellular protein folding in models of polyglutamine diseases. Science. 311:1471–1474. doi:10.1126/science.1124514.

Gidalevitz, T., T. Krupinski, S. Garcia, and R.I. Morimoto. 2009. Destabilizing protein polymorphisms in the genetic background direct phenotypic expression of mutant SOD1 toxicity. PLoS Genet. 5:e1000399. doi:10.1371/journal.pgen.1000399.

Gillis, J., S. Schipper-Krom, K. Juenemann, A. Gruber, S. Coolen, R. Van Den Nieuwendijk, H. Van Veen, H. Overkleeft, J. Goedhart, H.H. Kampinga, and E.A. Reits. 2013. The DNAJB6 and DNAJB8 protein chaperones prevent intracellular aggregation of polyglutamine peptides. J. Biol. Chem. 288:17225–17237. doi:10.1074/jbc.M112.421685.

Gross, L.A., G.S. Baird, R.C. Hoffman, K.K. Baldridge, and R.Y. Tsien. 2000. The structure of the chromophore within DsRed, a red fluorescent protein from coral. Proc. Natl. Acad. Sci. 97:11990–11995. doi:10.1073/pnas.97.22.11990.

Gupta, R., P. Kasturi, A. Bracher, C. Loew, M. Zheng, A. Villella, D. Garza, F.U. Hartl, and S. Raychaudhuri. 2011. Firefly luciferase mutants as sensors of proteome stress. Nat. Methods. 8:879–884. doi:10.1038/nmeth.1697.

Hageman, J., M.A. Rujano, M.A.W.H. van Waarde, V. Kakkar, R.P. Dirks, N. Govorukhina, H.M.J. Oosterveld-Hut, N.H. Lubsen, and H.H. Kampinga. 2010. A DNAJB Chaperone Subfamily with HDAC-Dependent Activities Suppresses Toxic Protein

Aggregation. Mol. Cell. 37:355–369. doi:10.1016/j.molcel.2010.01.001.

Hashimoto, M., E. Rockenstein, L. Crews, and E. Masliah. 2003. Role of Protein Aggregation in Mitochondrial Dysfunction and Neurodegeneration in Alzheimer's and Parkinson's Diseases. NeuroMolecular Med. 4:21–36. doi:10.1385/NMM:4:1-2:21.

Hazeki, N., T. Tukamoto, J. Goto, and I. Kanazawa. 2000. Formic acid dissolves aggregates of an N-terminal huntingtin fragment containing an expanded polyglutamine tract: applying to quantification of protein components of the aggregates. Biochem. Biophys. Res. Commun. 277:386–93. doi:10.1006/bbrc.2000.3682.

Hinault, M.P., A.F.H. Cuendet, R.U.H. Mattoo, M. Mensi, G. Dietler, H.A. Lashuel, and P. Goloubinoff. 2010. Stable -synuclein oligomers strongly inhibit chaperone activity of the Hsp70 system by weak interactions with J-domain co-chaperones. J. Biol. Chem. 285:38173–38182. doi:10.1074/jbc.M110.127753.

Hipp, M.S., S.H. Park, and U.U. Hartl. 2014. Proteostasis impairment in protein-misfolding and -aggregation diseases. Trends Cell Biol. 24:506–514. doi:10.1016/j.tcb.2014.05.003.

Kakkar, V., C. Månsson, E.P. de Mattos, S. Bergink, M. van der Zwaag, M.A.W.H. van Waarde, N.J. Kloosterhuis, R. Melki, R.T.P. van Cruchten, S. Al-Karadaghi, P. Arosio, C.M. Dobson, T.P.J. Knowles, G.P. Bates, J.M. van Deursen, S. Linse, B. van de Sluis, C. Emanuelsson, and H.H. Kampinga. 2016. The S/T-Rich Motif in the DNAJB6 Chaperone Delays Polyglutamine Aggregation and the Onset of Disease in a Mouse Model. Mol. Cell. 62:272–283. doi:10.1016/j.molcel.2016.03.017.

Kakkar, V., M. Meister-Broekema, M. Minoia, S. Carra, and H.H. Kampinga. 2014. Barcoding heat shock proteins to human diseases: looking beyond the heat shock response. Dis. Model. Mech. 7:421–434. doi:10.1242/dmm.014563.

Kakkar, V., L.C.B. Prins, and H.H. Kampinga. 2012. DNAJ Proteins and Protein Aggregation Diseases. Curr. Top. Med. Chem. 12:2479–2490. doi:10.2174/156802661121220004.

Kampinga, H.H., and S. Bergink. 2016. Heat shock proteins as potential targets for protective strategies in neurodegeneration. Lancet Neurol. 15:748–759. doi:10.1016/S1474-4422(16)00099-5.

Kim, Y.E., M.S. Hipp, A. Bracher, M. Hayer-Hartl, and F. Ulrich Hartl. 2013. Molecular Chaperone Functions in Protein Folding and Proteostasis. Annu. Rev. Biochem. 82:323–355. doi:10.1146/annurev-biochem-060208-092442.

Kim, Y.E., F. Hosp, F. Frottin, H. Ge, M. Mann, M. Hayer-Hartl, and F.U. Hartl. 2016. Soluble Oligomers of PolyQ-Expanded Huntingtin Target a Multiplicity of Key Cellular Factors. Mol. Cell. 63:950–964. doi:10.1016/j.molcel.2016.07.022.

Koyama, S., S. Arawaka, R. Chang-Hong, M. Wada, T. Kawanami, K. Kurita, M. Kato, M. Nagai, M. Aoki, Y. Itoyama, G. Sobue, P.H. Chan, and T. Kato. 2006. Alteration of familial ALS-linked mutant SOD1 solubility with disease progression: Its modulation by the proteasome and Hsp70. Biochem. Biophys. Res. Commun. 343:719–730. doi:10.1016/J.BBRC.2006.02.170.

Lashuel, H.A., and P.T. Lansbury. 2006. Are amyloid diseases caused by protein aggregates that mimic bacterial pore-forming toxins? Q. Rev. Biophys. 39:167. doi:10.1017/S0033583506004422.

Lin, M.T., and M.F. Beal. 2006. Mitochondrial dysfunction and oxidative stress in neurodegenerative diseases. Nature. 443:787–795. doi:10.1038/nature05292.

Liu, K.Y., Y.C. Shyu, B.A. Barbaro, Y.T. Lin, Y. Chern, L.M. Thompson, C.K.J. Shen, and J.L. Marsh. 2015. Disruption of the nuclear membrane by perinuclear inclusions of mutant huntingtin causes cell-cycle re-entry and striatal cell death in mouse and cell models of Huntington's disease. Hum. Mol. Genet. 24:1602–1616. doi:10.1093/hmg/ddu574.

Mateju, D., T.M. Franzmann, A. Patel, A. Kopach, E.E. Boczek, S. Maharana, H.O. Lee, S. Carra, A.A. Hyman, and S. Alberti. 2017. An aberrant phase transition of stress granules triggered by misfolded protein and prevented by chaperone function. EMBO J. 36:1669–1687. doi:10.15252/embj.201695957.

Matsumoto, G., S. Kim, and R.I. Morimoto. 2006. Huntingtin and mutant SOD1 form aggregate structures with distinct molecular properties in human cells. J. Biol. Chem. 281:4477–4485. doi:10.1074/jbc.M509201200.

Matsumoto, G., A. Stojanovic, C.I. Holmberg, S. Kim, and R.I. Morimoto. 2005. Structural properties and neuronal toxicity of amyotrophic lateral sclerosis-

associated Cu/Zn superoxide dismutase 1 aggregates. J. Cell Biol. 171:75–85. doi:10.1083/jcb.200504050.

Michalik, A., and C. Van Broeckhoven. 2003. Pathogenesis of polyglutamine disorders: aggregation revisited. Hum. Mol. Genet. 12:R173–R186. doi:10.1093/hmg/ddg295.

Miller, S.B.M., C. Ho, J. Winkler, M. Khokhrina, A. Neuner, M.Y.H. Mohamed, D.L. Guilbride, K. Richter, M. Lisby, E. Schiebel, A. Mogk, and B. Bukau. 2015. Compartment-specific aggregases direct distinct nuclear and cytoplasmic aggregate deposition. EMBO J. 34:778–97. doi:10.15252/embj.201489524.

Olzscha, H., S.M. Schermann, A.C. Woerner, S. Pinkert, M.H. Hecht, G.G. Tartaglia, M. Vendruscolo, M. Hayer-Hartl, F.U. Hartl, and R.M. Vabulas. 2011. Amyloid-like aggregates sequester numerous metastable proteins with essential cellular functions. Cell. 144:67–78. doi:10.1016/j.cell.2010.11.050.

Park, S.H., Y. Kukushkin, R. Gupta, T. Chen, A. Konagai, M.S. Hipp, M. Hayer-Hartl, and F.U. Hartl. 2013. PolyQ proteins interfere with nuclear degradation of cytosolic proteins by sequestering the Sis1p chaperone. Cell. 154:134–145. doi:10.1016/j.cell.2013.06.003.

Polling, S., Y.F. Mok, Y.M. Ramdzan, B.J. Turner, J.J. Yerbury, A.F. Hill, and D.M. Hatters. 2014. Misfolded polyglutamine, polyalanine, and superoxide dismutase 1 aggregate via distinct pathways in the cell. J. Biol. Chem. 289:6669–6680. doi:10.1074/jbc.M113.520189.

Prudencio, M., P.J. Hart, D.R. Borchelt, and P.M. Andersen. 2009. Variation in aggregation propensities among ALS-associated variants of SOD1: Correlation to human disease. Hum. Mol. Genet. 18:3217–3226. doi:10.1093/hmg/ddp260.

Qualls, D.A., M. Prudencio, B.L.T. Roberts, K. Crosby, H. Brown, and D.R. Borchelt. 2013. Features of wild-type human SOD1 limit interactions with misfolded aggregates of mouse G86R Sod1. Mol. Neurodegener. 8:46. doi:10.1186/1750-1326-8-46.

Ray, S.S., R.J. Nowak, K. Strokovich, R.H. Brown, T. Walz, and P.T. Lansbury. 2004. An Intersubunit Disulfide Bond Prevents in Vitro Aggregation of a Superoxide Dismutase-1 Mutant Linked to Familial Amytrophic Lateral Sclerosis. Biochemistry. 43:4899–4905. doi:10.1021/bi030246r.

Ross, C.A., and M.A. Poirier. 2004. Protein aggregation and neurodegenerative disease. Nat. Med. 10:S10. doi:10.1038/nm1066.

Rujano, M.A., H.H. Kampinga, and F.A. Salomons. 2007. Modulation of polyglutamine inclusion formation by the Hsp70 chaperone machine. Exp. Cell Res. 313:3568–3578. doi:10.1016/j.yexcr.2007.07.034.

Soto, C. 2003. Unfolding the role of protein misfolding in neurodegenerative diseases. Nat. Rev. Neurosci. 4:49–60. doi:10.1038/nrn1007.

Suhr, S.T., M.C. Senut, J.P. Whitelegge, K.F. Faull, D.B. Cuizon, and F.H. Gage. 2001. Identities of sequestered proteins in aggregates from cells with induced polyglutamine expression. J. Cell Biol. 153:283–294. doi:10.1083/jcb.153.2.283.

Takeuchi, H., Y. Kobayashi, T. Yoshihara, and J.-I. Niwa. 2002. Hsp70 and Hsp40 improve neurite outgrowth and suppress intracytoplasmic aggregate formation in cultured neuronal cells expressing mutant SOD1. Brain Res. 949:11–22.

Tyedmers, J., A. Mogk, and B. Bukau. 2010. Cellular strategies for controlling protein aggregation. Nat. Rev. Mol. Cell Biol. 11:777–788. doi:10.1038/nrm2993.

Vonk, W.I.M., V. Kakkar, P. Bartuzi, D. Jaarsma, R. Berger, M.H. Hofker, L.W.J. Klomp, C. Wijmenga, H.H. Kampinga, and B. Van De Sluis. 2014. The Copper Metabolism MURR1 Domain protein 1 (COMMD1) modulates the aggregation of misfolded protein species in a client-specific manner. PLoS One. 9:e92408. doi:10.1371/journal.pone.0092408.

Wang, J., G.W. Farr, C.J. Zeiss, D.J. Rodriguez-Gil, J.H. Wilson, K. Furtak, D.T. Rutkowski, R.J. Kaufman, C.I. Ruse, J.R. 3rd Yates, S. Perrin, M.B. Feany, and A.L. Horwich. 2009. Progressive aggregation despite chaperone associations of a mutant SOD1-YFP in transgenic mice that develop ALS. Proc. Natl. Acad. Sci. U. S. A. 106:1392–1397. doi:10.1073/pnas.0813045106.

Wang, Y., A.B. Meriin, C.E. Costello, and M.Y. Sherman. 2007. Characterization of proteins associated with polyglutamine aggregates: a novel approach towards isolation of aggregates from protein conformation disorders. Prion. 1:128–135. doi:10.4161/pri.1.2.4440.

Weisberg, S.J., R. Lyakhovetsky, A. -c. Werdiger, A.D. Gitler, Y. Soen, and D. Kaganovich. 2012.

Compartmentalization of superoxide dismutase 1 (SOD1G93A) aggregates determines their toxicity. Proc. Natl. Acad. Sci. 109:15811–15816. doi:10.1073/pnas.1205829109.

Wigley, C.W., R.P. Fabunmi, M.G. Lee, C.R. Marino, S. Muallem, G.N. DeMartino, and P.J. Thomas. 1999. Dynamic association of proteasomal machinery with the centrosome. J. Cell Biol. 145:481–490. doi:10.1083/jcb.145.3.481.

Woerner, A.C., F. Frottin, D. Hornburg, L.R. Feng, F. Meissner, M. Patra, J. Tatzelt, M. Mann, K.F. Winklhofer, F.U. Hartl, and M.S. Hipp. 2016. Cytoplasmic protein aggregates interfere with nucleocytoplasmic transport of protein and RNA. Science. 351:173–176. doi:10.1126/science.aad2033.

Wyttenbach, A., J. Carmichael, J. Swartz, R.A. Furlong, Y. Narain, J. Rankin, and D.C. Rubinsztein. 2000. Effects of heat shock, heat shock protein 40 (HDJ-2), and proteasome inhibition on protein aggregation in cellular models of Huntington's disease. Proc. Natl. Acad. Sci. U. S. A. 97:2898–2903. doi:10.1073/pnas.97.6.2898.

Xie, W., O.W. Wan, and K.K.K. Chung. 2010. New insights into the role of mitochondrial dysfunction and protein aggregation in Parkinson's disease. Biochim. Biophys. Acta - Mol. Basis Dis. 1802:935–941. doi:10.1016/j.bbadis.2010.07.014.

Yu, A., Y. Shibata, B. Shah, B. Calamini, D.C. Lo, and R.I. Morimoto. 2014. Protein aggregation can inhibit clathrin-mediated endocytosis by chaperone competition. Proc. Natl. Acad. Sci. 111:E1481–E1490. doi:10.1073/pnas.1321811111.

Supplementary Information

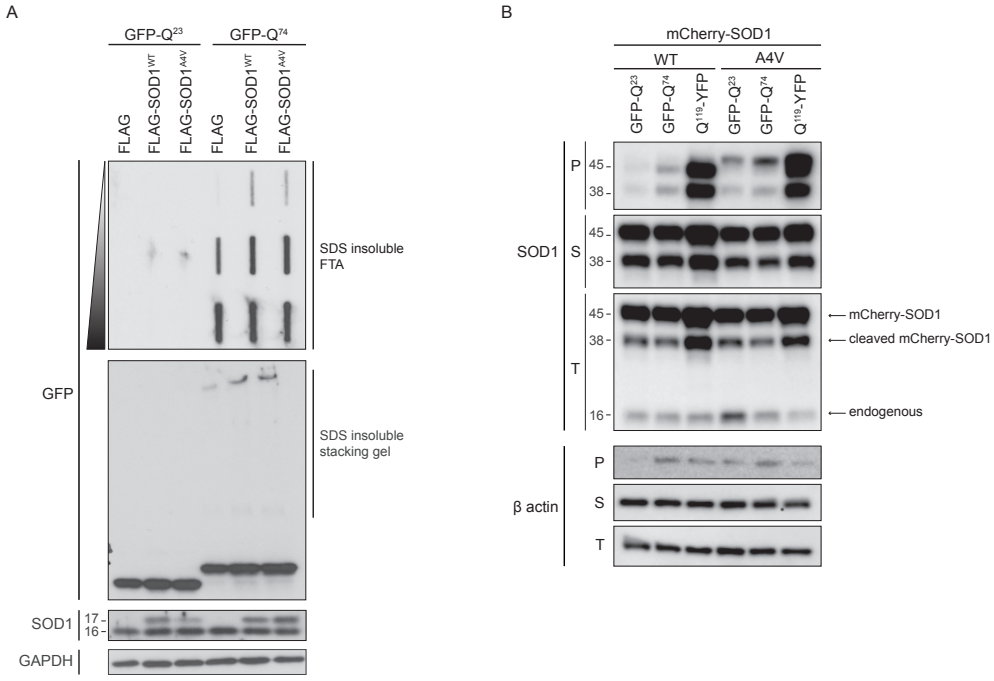

Figure S1. SOD1^{A4V} does not have an effect on Q^{74} aggregation but Q^{74} and Q^{119} increase SOD1^{A4V} aggregation. **(A)** Western blots of filter trap assay (FTA) and total cell lysates of cells co-expressing either GFP-Q^{23} or -Q^{74} with FLAG-control, FLAG-SOD1^{WT} or FLAG-SOD1^{A4V} for 48 hours. SDS insoluble fractions of polyQ are shown in both FTA, with increasing 5-fold dilutions from bottom to top, and stacking gel blots with GFP antibody. GFP, SOD1 and GAPDH (loading control) were used for the total cell lysates. **(B)** NP40 fractionation of HEK293 cells co-expressing GFP-Q^{23}, GFP-Q^{43} or Q^{119}-YFP and mCherry-tagged SOD1^{WT} or SOD1^{A4V}. Total cell lysates (T), NP40-soluble (S), NP40-insoluble (P) of SOD1 and actin (loading control) are shown.

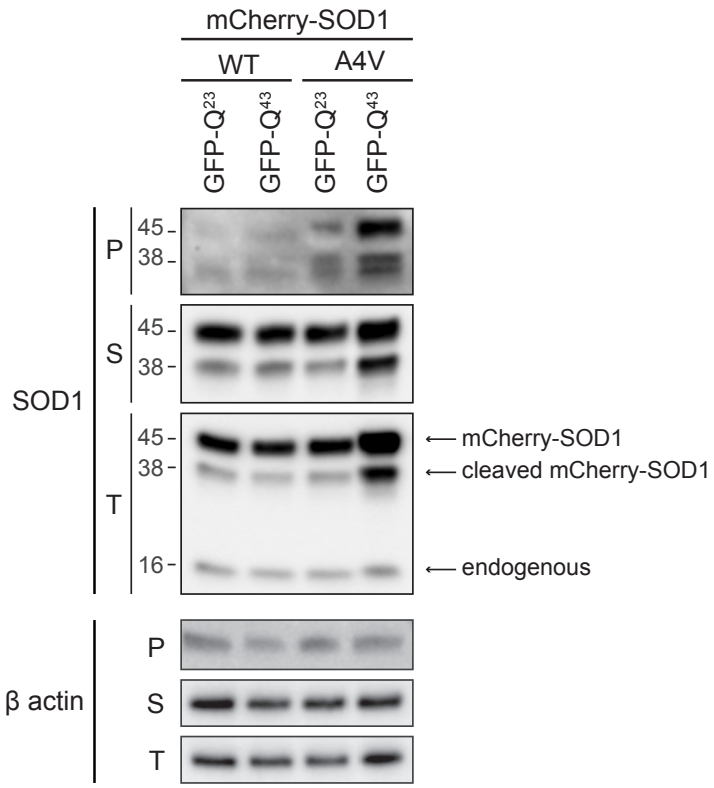

Figure S2. **Q^{43} expressed for 72 hours can enhance $SOD1^{A4V}$ aggregation.** NP40 fractionation of HEK293 cells co-expressing GFP-tagged Q^{23} or Q^{43} for 72 hours and mCherry-tagged $SOD1^{WT}$ or $SOD1^{A4V}$ for 48 hours. Total cell lysates (T), NP40-soluble (S), NP40-insoluble (P) of SOD1 and actin (loading control) are shown.

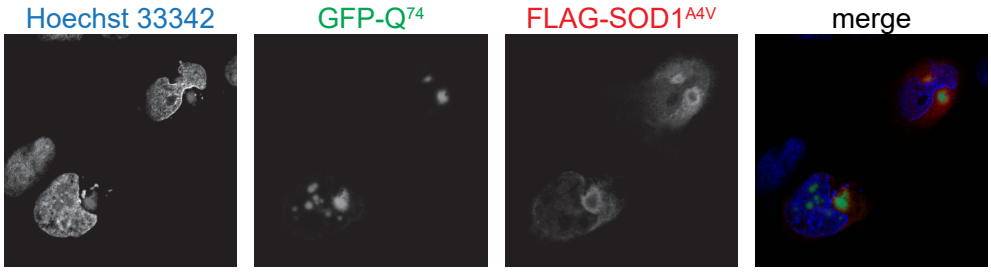

Figure S3. $SOD1^{A4V}$ can accumulate as a ring around large polyQ aggregates. U2OS cells co-expressing GFP-tagged Q74 (green) with FLAG-$SOD1^{A4V}$ (red) for 48 hours detected by fluorescence confocal microscopy. FLAG tagged $SOD1^{A4V}$ is stained anti-FLAG and Alexa 633 secondary antibody. Hoechst 33342 (blue) is used to stain nuclei. A single focal plane is shown as an individual z-stack image.

Table S1. Effect of chaperone expression on polyQ or mutant SOD1 aggregation.

Data from Hageman et al, 2010 (polyQ) and **Chapter 2** ($SOD1^{A4V}$). Effect on aggregation is calculated from aggregation percentage relative to control: decrease is <90% (green), no change is 90-110% (grey), increase is >110% aggregation (orange).

Chaperones			PolyQ			$SOD1^{A4V}$		
			-	↓	↑	-	↓	↑
HSP110/HSPH		HSPH1						
		HSPH2						
		HSPH3						
Hsp70/HSPA		HSPA1A						
		HSPA1L						
		HSPA2						
		HSPA5						
		HSPA6						
		HSPA8						
		HSPA9						
DNAJ	DNAJA	HSP14						
		DNAJA1						
		DNAJA2						
		DNAJA3						
	DNAJB	DNAJA4						
		DNAJB1						
		DNAJB2a						
		DNAJB2b						
		DNAJB3						
		DNAJB4						
		DNAJB5						
		DNAJB6a						
		DNAJB6b						
		DNAJB7						
		DNAJB8						
		DNAJB9						

Table S2. List of primers used for cloning

Primer name	Sequence 5' to 3'		Used for	Template
ecoRV xhoI SOD for	CAGTTCGATATCGCTCGAGCTGCGACGAAGG-CCGTGTGCGTGCTG	for	EcoRV-XhoI-SOD1	pEBB-FLAG-SOD1
SOD bamHI notI rev	CGGACGCGGCCGCGGATCCTTATTGGGCG-ATCCCAATTACACC	rev	BamHI-NotI-SOD1	pEBB-FLAG-SOD1
for hind-cherry	CGTCCAAGCTTATGGTGAGCAAGGGCGAG-GAG	for	HindIII-mCherry	pcDNA3.1(+)-mCherry-alpha tubulin
rev cherry-ecoRV	GCACTGATATCCTTGTACAGCTCGTCCATGC	rev	mCherry-EcoRV	pcDNA3.1(+)-mCherry-alpha tubulin
for mut sod a4v	GCGACGAAGGTCGTGTGCGTGCTGAAG	for	SOD1-A4V mutagenesis	pcDNA5-FRT/TO-mCherry-SOD1
rev mut sod a4v	CTTCAGCACGCACACGACCTTCGTCGC	rev	SOD1-A4V mutagenesis	pcDNA5-FRT/TO-mCherry-SOD1